

Bounds on mean energy in the Kuramoto–Sivashinsky equation computed using semidefinite programming

David Goluskin^{1,2,*} and Giovanni Fantuzzi³

¹Department of Mathematics and Statistics, University of Victoria, Victoria, BC, V8P 5C2, Canada

²Department of Mathematics, University of Michigan, Ann Arbor, MI 48109, USA

³Department of Aeronautics, Imperial College London, South Kensington Campus, London, SW7 2AZ, UK

October 11, 2024

Abstract

We present methods for bounding infinite-time averages in dynamical systems governed by nonlinear PDEs. The methods rely on auxiliary functionals, which are similar to Lyapunov functionals but satisfy different inequalities. The inequalities are enforced by requiring certain expressions to be sums of squares of polynomials, and the optimal choice of auxiliary functional is posed as a semidefinite program (SDP) that can be solved computationally. To formulate these SDPs we approximate the PDE by truncated systems of ODEs and proceed in one of two ways. The first approach is to compute bounds for the ODE systems, increasing the truncation order until bounds converge numerically. The second approach incorporates the ODE systems with analytical estimates on their deviation from the PDE, thereby using finite truncations to produce bounds for the full PDE. We apply both methods to the Kuramoto–Sivashinsky equation. In particular, we compute upper bounds on the spatiotemporal average of energy by employing polynomial auxiliary functionals up to degree six. The first approach is used for most computations, but a subset of results are checked using the second approach, and the results agree to high precision. These bounds apply to all odd solutions of period $2\pi L$, where L is varied. Sharp bounds are obtained for $L \leq 10$, and trends suggest that more expensive computations would yield sharp bounds at larger L also. The bounds are known to be sharp (to within 0.1% numerical error) because they are saturated by the simplest nonzero steady states, which apparently have the largest mean energy among all odd solutions. Prior authors have conjectured that mean energy remains $O(1)$ for $L \gg 1$ since no particular solutions with larger energy have been found. Our bounds constitute the first positive evidence for this conjecture, albeit up to finite L , and offer guidance for analytical proofs.

*Email: goluskin@uvic.ca

1 Introduction

The one-dimensional Kuramoto–Sivashinsky equation (KSE) has attracted significant attention not only as a physical model [29, 30, 35, 50, 51] but also as a bridge between low-dimensional chaotic systems and high-dimensional spatiotemporal chaos, including fluid turbulence [23, 24, 26]. Here we consider mean-zero solutions $u(x, t)$ with spatial period $2\pi L$, where L is a parameter:

$$\begin{aligned} u_t &= -u u_x - u_{xx} - u_{xxxx}, \\ u(x, t) &= u(x + 2\pi L, t), \\ u(x, 0) &= u_0(x), \quad \int u_0(x) \, dx = 0. \end{aligned} \tag{1}$$

For simplicity we restrict most of our analysis to the subspace of odd solutions where $u(-x, t) = -u(x, t)$. All spatial integrals are over $[-\pi L, \pi L]$ unless otherwise noted. Solutions exist for all $t \geq 0$ and have strong regularity properties including finiteness of all Sobolev norms [39]. Simulations of the KSE display spatiotemporal chaos of increasingly large dimension as the spatial period is raised [27, 49].

Our objective is twofold: to develop methods for bounding average quantities governed by nonlinear PDEs, and to produce novel results for the KSE using these methods. The methods follow an approach used commonly in the study of dynamics: constructing a functional that, by satisfying suitable inequalities, implies the desired result. Here the choice of functional is optimized with computer assistance. This is done by replacing all relevant inequalities with constraints that require certain polynomials to be representable as sums of squares. The resulting convex optimization problem can be translated into a semidefinite program (SDP) and solved numerically. Such SDP-based methods have produced various mathematical statements about nonlinear ODEs, including verification of nonlinear stability [2, 43, 46], estimation of attractor basins [22], and bounds on time averages [5, 12, 17]. Here we extend methods for bounding time averages to the PDE setting. Our approach relies on the construction of *auxiliary functionals*, which satisfy particular conditions that imply the desired bounds. As explained in §2, these conditions are related to but not the same as conditions on Lyapunov functionals, which can be used to bound instantaneous quantities or prove nonlinear stability.

The quantity on which we focus is the spatially averaged energy in the KSE,

$$\mathcal{E}(t) := \mathfrak{f} u(x, t)^2 \, dx, \tag{2}$$

where \mathfrak{f} denotes the spatial average $\frac{1}{2\pi L} \int_{-\pi L}^{\pi L}$. Note that past authors have discussed the energy in various terms, including \mathcal{E} , $\frac{1}{2}\mathcal{E}$, and $\|u\|_2 = (\int u^2 \, dx)^{1/2}$. Here we compute upper

bounds on the spatiotemporal average of the energy,

$$\bar{\mathcal{E}} := \limsup_{T \rightarrow \infty} \frac{1}{T} \int_0^T \mathcal{E}(t) dt, \quad (3)$$

for various L . At each L we seek an upper bound $\bar{\mathcal{E}} \leq B$ that is as small as possible. The scaling of our bounds with increasing L has implications for the long-standing challenge to analytically prove bounds that scale optimally when $L \gg 1$.

Upper bounds on the energy have been pursued for several decades as part of a larger conjecture dating to the 1980s [49, 56], which asserts that various average quantities scale intensively in large domains—that is, they are independent of L when $L \gg 1$. Intensive scaling would be confirmed for a quantity of interest if one could prove upper and lower bounds that are $O(1)$ for $L \gg 1$. The trivial lower bound of $\bar{\mathcal{E}} \geq 0$ cannot be improved upon for general initial conditions since it is saturated by the $u = 0$ state. On the other hand, there is hope of constructing $O(1)$ upper bounds since no solutions displaying larger scaling have been reported. To date, $O(1)$ upper bounds have been proved only for steady solutions [34], and logarithmic-in- L upper bounds have been proved only for spatiotemporal averages of $(|\partial_x|^\alpha u)^2$ with $1/3 \leq \alpha \leq 2$ [16, 42]. The best bounds proven for mean energy grow as powers of L .

Most bounds on energy in the KSE have focused on its instantaneous value on the attractor,

$$\mathcal{E}_\infty := \limsup_{t \rightarrow \infty} \mathcal{E}(t). \quad (4)$$

Upper bounds on \mathcal{E}_∞ apply to the time average $\bar{\mathcal{E}}$, but not vice versa, since $\bar{\mathcal{E}} \leq \mathcal{E}_\infty$. The first result, proved in the 1980s, was that $\mathcal{E}_\infty \leq O(L^4)$ for odd solutions [39]. Later this was extended to all solutions of (1) and improved to $\mathcal{E}_\infty \leq O(L^2)$ [3, 6, 19]. All of these results were proved using quadratic Lyapunov functionals. Bounds that grow more slowly than $O(L^2)$ have been proved by Otto and coworkers using an “entropy method” in which solutions of the KSE are estimated using entropy solutions of the inviscid Burgers equation. Their bounds on the instantaneous [15] and time-averaged [16, 42] energy are currently the best available in the $L \gg 1$ limit:

$$\mathcal{E}_\infty \leq o(L) \quad \text{and} \quad \bar{\mathcal{E}} \leq O(L^{2/3+}). \quad (5)$$

Here we focus on bounding $\bar{\mathcal{E}}$, rather than \mathcal{E}_∞ , for two reasons. First, it is easier in the time-averaged case to confirm that bounds are sharp because, it turns out, they are saturated by simple equilibria. Second, time-averaged bounds are easier to optimize computationally because the optimization problem is convex, as described in the next section.

Despite the success of the entropy method, which relies on particular features of the KSE, there are compelling reasons to continue developing the earlier approach. Lyapunov functionals and auxiliary functionals, which can be used to bound \mathcal{E}_∞ and $\bar{\mathcal{E}}$, respectively,

are very broadly applicable to nonlinear PDEs. Furthermore, our results for the KSE suggest a way to possibly improve upon (5). It has been argued that $\mathcal{E}_\infty \leq O(L^2)$ is the best bound provable using quadratic Lyapunov functionals [3, 55]. Indeed, using SDPs to optimize quadratic Lyapunov functionals improves the bounds of [3] but not their $O(L^2)$ scaling [13]. We likewise find for the time-averaged problem that quadratic auxiliary functionals give $\bar{\mathcal{E}} \leq O(L^2)$. However, we also produce better bounds on $\bar{\mathcal{E}}$ here using auxiliary functionals that are not quadratic. In particular, we use SDP-based computations to construct quartic and sextic polynomial auxiliary functionals. Since the restriction to quadratic functionals is equivalent to the ‘‘background method’’ used in past studies of the KSE and numerous fluid dynamical models [4], the present work is a generalization of the background method.

Our computational approaches require approximating the PDE by systems of ODEs that are derived from the PDE by Galerkin truncation. Methods for using SDP computations to bound time averages in ODE systems have been demonstrated previously [5, 12, 17], albeit only for systems of dimension 9 or fewer. One option is to approximate bounds for the PDE by computing bounds for ODE truncations, increasing the truncation dimension until the bounds converge. A second option is to compute bounds for the PDE using an ODE truncation of fixed size, along with analytical estimates controlling the difference between solutions to the ODE system and the PDE. The bound for the PDE is computed by solving an SDP that incorporates the truncated system and the analytical estimates. Here we apply both approaches to the KSE. Each approach produces bounds for various L that are within 0.1% of being sharp. The first approach does so with less computational cost, so most of our results have been computed in this way.

Section 2 describes how auxiliary functionals can be used to bound spatiotemporal averages in PDEs, and how the analysis can be carried out with computer assistance by solving SDPs. The relationship to Lyapunov functionals is explained, and the methodology is tailored to the KSE. Section 3 reviews the bifurcation structure of the KSE as needed to judge the quality of our bounds, which are presented in §4. In §5 we offer several conjectures about the KSE motivated by our computations, followed by conclusions about our methodology in general. Appendices provide details on computational methods and results.

2 Auxiliary functionals and Lyapunov functionals

Bounds on time averages for many different PDEs have been proved using auxiliary functionals, although often the proofs are not presented in this framework, and the choice of functional is not explicit. The framework is summarized in §2.1, and the corresponding framework for bounding instantaneous values on attractors using Lyapunov functionals is discussed in §2.2. As a simple example for the KSE, §2.3 describes quadratic auxiliary and Lyapunov functionals, which are tantamount to using the background method. Section

2.4 describes a general framework for polynomial auxiliary functionals of any degree. The construction of such functionals can be posed as a polynomial optimization problem that is equivalent to an SDP. This is described in §2.4.1 for Galerkin truncations of PDEs and in §2.4.2 for the full PDEs. In §2.5 both approaches are formulated for the KSE in particular.

2.1 Auxiliary functionals

Consider an autonomous PDE,

$$u_t(x, t) = F(u(x, t)), \quad (6)$$

whose righthand side $F(u)$ involves differentiation in $x \in \mathbb{R}^m$. Assume that solutions remain in some function space \mathcal{U} , meaning $u(\cdot, t) \in \mathcal{U}$ for all $t \geq 0$. Suppose we are interested in a real-valued functional $\Phi(u(\cdot, t))$ that remains bounded along each solution trajectory. Its infinite-time average $\overline{\Phi}$ may depend on the trajectory along which it is evaluated. Our objective is to bound the possible values of $\overline{\Phi}$. This can be done using an *auxiliary functional*, $V : \mathcal{U} \rightarrow \mathbb{R}$, that is absolutely continuous, differentiable, and remains bounded along trajectories. The conditions on V ensure that the infinite-time average $\overline{\frac{d}{dt}V}$ vanishes, so along each solution $u(x, t)$ of the PDE,

$$\overline{\Phi} = \overline{\Phi + \frac{d}{dt}V}. \quad (7)$$

Let $D_V : \mathcal{U} \rightarrow \mathbb{R}$ be the time-independent functional that is equal to $\frac{d}{dt}V(u(\cdot, t))$ along all trajectories. An expression for $D_V(u)$ must be deduced from the dynamics (6). For instance if $V(u) = \int u^2 dx$ and the PDE solution $u(x, t)$ is sufficiently regular, then $D_V(u) = 2 \int u F(u) dx$. To prove an upper bound $\overline{\Phi} \leq B$ it suffices to find a V such that $\Phi(u) + D_V(u) \leq B$ for all $u \in \mathcal{U}$. This condition implies $\Phi(u(\cdot, t)) + \overline{\frac{d}{dt}V(u(\cdot, t))} \leq B$ on all trajectories at all times, which implies the desired bound on $\overline{\Phi}$ via the identity (7). For convenience we rearrange the sufficient condition for $\overline{\Phi} \leq B$ into a standard form:

$$S(u) := B - \Phi(u) - D_V(u) \geq 0 \quad \forall u \in \mathcal{U}. \quad (8)$$

The PDE enters the functional $S(u)$ only through the derivation of $D_V(u)$.

If all auxiliary functionals V in some class \mathcal{V} are known to be admissible, meaning $\overline{\frac{d}{dt}V}$ vanishes on all PDE trajectories, we can optimize over \mathcal{V} to minimize the bound:

$$\overline{\Phi} \leq \inf_V B \quad \text{s.t.} \quad V \in \mathcal{V}, \quad S(u) \geq 0 \quad \forall u \in \mathcal{U}. \quad (9)$$

If the set \mathcal{V} is convex, then the righthand side of (9) is a convex optimization problem. This fact is central to our SDP-based methods for optimizing V computationally. For

broad families of PDEs [52] and ODEs [53], there exists a convex class \mathcal{V} such that the righthand side of (9) is guaranteed to produce arbitrarily sharp bounds:

$$\sup_{u(x,t) \text{ solves (6)}} \bar{\Phi} = \inf_V B \quad \text{s.t.} \quad V \in \mathcal{V}, \quad S(u) \geq 0 \quad \forall u \in \mathcal{U}. \quad (10)$$

In practice it may or may not be tractable to optimize over a \mathcal{V} that is large enough to give a bound B saturating, or near saturating, the above equality. If not, it still is desirable to optimize bounds over a numerically tractable subset of \mathcal{V} .

2.2 Lyapunov functionals

Often when studying a dynamical PDE (6), the objective is to bound instantaneous values $\Phi(u(\cdot, t))$ on a global attractor, rather than the time average $\bar{\Phi}$. Suppose we seek an upper bound on the long-time maximum defined on each trajectory $u(x, t)$ by

$$\Phi_\infty := \limsup_{t \rightarrow \infty} \Phi(u(\cdot, t)). \quad (11)$$

An upper bound $\Phi_\infty \leq C$ for all trajectories can be proved by finding some functional $W : \mathcal{U} \rightarrow \mathbb{R}$, and the corresponding functional $D_W : \mathcal{U} \rightarrow \mathbb{R}$ that is equal to $\frac{d}{dt}W(u(\cdot, t))$ along all PDE trajectories, such that

$$\Phi(u) \leq W(u), \quad (12)$$

$$a D_W(u) \leq C - W(u) \quad (13)$$

for some $a > 0$. We regard $W(u)$ as a kind of Lyapunov functional, although in some cases it can be negative. The above conditions are not the only ones that can be used to bound Φ_∞ , but they are among the simplest. Condition (13) implies $W_\infty \leq C$ by Gronwall's inequality, provided that $\frac{d}{dt}W(u(\cdot, t))$ is continuous along all trajectories, and then (12) implies $\Phi_\infty \leq C$.

For any Lyapunov functional W that proves $\Phi_\infty \leq C$ via conditions (12)–(13), the auxiliary functional $V(u) = a W(u)$ proves the same upper bound $\bar{\Phi} \leq C$ via condition (8). The converse is not true; if $V(u)$ satisfies (8) for a given bound, $W(u) = V(u)/a$ need not satisfy (12)–(13) for the same bound. This is consistent with the fact that $\bar{\Phi} \leq \Phi_\infty$.

As with the optimization of time-averaged bounds in (9), it is natural to seek the smallest bound C by optimizing W within some convex class, subject to (12)–(13). This optimization is convex for fixed a , but the joint optimization over a and W is not convex because a and D_W are multiplied in condition (13). This difficulty is absent in the optimization (9) over auxiliary functionals, which is one reason we focus here on bounding time averages rather than instantaneous quantities.

2.3 Quadratic auxiliary functionals for the KSE

In the case of the KSE, the simplest auxiliary functionals giving finite bounds on $\bar{\mathcal{E}}$ are quadratic functionals in the class

$$\mathcal{V} = \left\{ c \int u^2 dx + P(u) \mid c \in \mathbb{R}, P \in H^{2*} \right\}, \quad (14)$$

where H^{2*} is the dual of the Sobolev space H^2 , meaning $P : H^2 \rightarrow \mathbb{R}$ is a continuous linear functional. All $V \in \mathcal{V}$ are bounded along mean-zero solutions of the KSE, so it remains only to enforce $S(u) \geq 0$. This requires $D_V(u)$ to be bounded above, which is why its quadratic term is constrained to the form in (14). A quadratic term in V generically leads to a cubic term in D_V since the nonlinearity of the KSE is quadratic. This is not the case for the quadratic term of (14) since the nonlinearity of the KSE conserves energy:

$$\frac{d}{dt} \frac{1}{2} \int u^2 dx = \int uu_t dx = - \int u(uu_x + u_{xx} + u_{xxxx}) dx = \int (u_x^2 - u_{xx}^2) dx. \quad (15)$$

An equivalent way to ensure that $V \in \mathcal{V}$ is to use the ansatz

$$V(u) = \frac{\alpha}{2} \int (u - \zeta)^2 dx. \quad (16)$$

Any $P(u)$ in (14) can be represented by a corresponding $\zeta \in H^2$, as guaranteed by the Riesz representation theorem, and the u -independent integral $\int \zeta^2 dx$ is irrelevant since it does not enter $\frac{d}{dt} V$. Using the ansatz (16) is an instance of the background method [10], so called because $u - \zeta$ is the deviation of u from a “background” function $\zeta(x)$.

After evaluation of $\frac{d}{dt} V$ and integration by parts, the functional S defined by (8) becomes

$$S(u) = \int [\alpha u_{xx}^2 - \alpha u_x^2 + (\frac{1}{2}\alpha\zeta_x - 1) u^2] dx + \int (\alpha\zeta_x u_x - \alpha\zeta_{xx} u_{xx}) dx + B. \quad (17)$$

We regard the tunable variables as α and $\alpha\zeta$, as opposed to α and ζ , since S is jointly convex in the former pair. For quadratic V , the optimization problem (9) for the best upper bound on $\bar{\mathcal{E}}$ in the KSE is

$$\begin{aligned} \bar{\mathcal{E}} \leq \inf_{\substack{\alpha, \alpha\zeta \\ \zeta \in H^2}} B & \quad \text{s.t.} \quad \alpha \in \mathbb{R} \\ & \quad (17) \geq 0 \quad \forall u \in H^2. \end{aligned} \quad (18)$$

Numerical solutions of the righthand minimization are $O(L^2)$ for $L \gg 1$, as reported in §4, and Appendix C gives examples of optimal $\zeta(x)$ for several domain sizes. However, if upper bounds smaller than $O(L^2)$ are to be proved using auxiliary functionals, we must generalize beyond the quadratic class (14).

Remark 1. Like auxiliary functionals, every quadratic Lyapunov functional must have a leading term proportional to $\int u^2 dx$ in order for condition (13) to be possible. Thus any quadratic Lyapunov functional can be expressed as in (16), up to addition of another constant. This is the framework that past authors have used when proving bounds on \mathcal{E}_∞ with Lyapunov functionals [3, 6, 13, 19, 39]. Successively better analytical constructions for ζ led to the $O(L^2)$ bounds [3]. Still better ζ computed using SDPs improved these bounds but not their scaling [13]. The full optimization over quadratic Lyapunov functionals subject to (12)–(13) has not been solved, but we suspect that it would produce $O(L^2)$ bounds also. Optimizing over higher-degree functionals, as we do here for the time-averaged problem, remains a topic for future work.

Remark 2. Most applications of the background method to PDEs—that is, of quadratic auxiliary functionals with leading terms proportional to energy—have been to the Navier–Stokes equations and related fluid dynamical systems (e.g., [7, 8, 18, 38, 48]). Since these equations have the same type of nonlinear term as the KSE, any term of V that is quadratic in the velocity field $\mathbf{u}(\mathbf{x}, t)$ must be proportional to the energy in order for D_V to be quadratic instead of cubic. Therefore such V can be written as

$$V(\mathbf{u}) = c \int_{\Omega} |\mathbf{u} - \zeta|^2 d\mathbf{x}, \quad (19)$$

possibly with additional terms involving other variables such as temperature. As pointed out by Chernyshenko [4], such quadratic auxiliary functionals underlie all past uses of the background method to bound time averages, although in many cases V was not given explicitly.

2.4 Auxiliary functionals of any polynomial degree

Having illustrated the use of quadratic auxiliary functionals for the KSE, let us return to the general PDE (6) and the optimization (9) over auxiliary functionals. Our aim is to formulate bounding problems for higher-than-quadratic auxiliary functionals that can be solved efficiently using polynomial optimization. In order for polynomial optimization to be directly applicable, we restrict our discussion to dynamics and quantities to bound— $F(u)$ and $\Phi(u)$ —that are polynomial in u and its spatial derivatives. The KSE and its mean energy have this property. We also restrict attention to auxiliary functionals with polynomial dependence on u . Whereas quadratic functionals of the restricted form (14) can be represented by a constant c and background function ζ , representations of higher-degree V are more complicated. Here we let V be a polynomial function of the projections of u onto an L^2 -orthonormal basis $\{u_n(x)\}_{n \geq 1}$. That is, we expand

$$u(x, t) = \sum_{n=1}^{\infty} a_n(t) u_n(x). \quad (20)$$

and consider

$$V(u) = V(a_1, a_2, \dots), \quad (21)$$

where the righthand side is a polynomial function of the expansion coefficients $\{a_n\}_{n \geq 1}$.

While for analytical purposes V might include an infinite number of monomials, for computational purposes we must optimize V over a finite-dimensional space. A relatively simple approach, described in §2.4.1, is to truncate the Galerkin expansion (20) after N modes, replace the PDE with its projection onto these modes, and let $V = V(a_1, \dots, a_N)$. An alternate approach which does not require truncating the PDE, described in §2.4.2, is to let V depend not only on (a_1, \dots, a_N) but also on functionals of the “tail” of the expansion of u .

2.4.1 Bounds for truncated ODE systems

To approximate the PDE (6) by a finite-dimensional system we employ an N -mode Galerkin projection. Truncating the expansion (20) after the first N terms and integrating each basis function $u_n(x)$ against the PDE yields a system of ODEs of the form

$$\frac{d}{dt} \mathbf{a} = \mathbf{f}(\mathbf{a}), \quad (22)$$

where $\mathbf{a} = (a_1, \dots, a_N)$ is the vector of mode amplitudes, and each component of $\mathbf{f}(\mathbf{a})$ is a polynomial since the PDE has polynomial dependence on u . We likewise replace the quantity to be bounded with its N -mode truncation, $\Phi_N(\mathbf{a})$, and seek bounds on the time average $\bar{\Phi}_N$.

If all trajectories of the truncated system (22) remain bounded, then bounds on $\bar{\Phi}_N$ can be computed using existing SDP-based methods for ODEs [5, 12, 17]. The chain rule gives $\frac{d}{dt} V(\mathbf{a}) = \mathbf{f} \cdot \nabla V(\mathbf{a})$, so the bounding condition (8) that proves $\bar{\Phi}_N \leq B$ becomes the polynomial inequality

$$S(\mathbf{a}) = B - \Phi_N(\mathbf{a}) - \mathbf{f}(\mathbf{a}) \cdot \nabla V(\mathbf{a}) \geq 0 \quad \forall \mathbf{a} \in \mathbb{R}^N. \quad (23)$$

Even with computer assistance it is prohibitively difficult in general to decide whether a polynomial is nonnegative—the computational complexity is NP-hard [37]. We thus employ a standard technique in polynomial optimization [47]: replace the condition $S(\mathbf{a}) \geq 0$ with the stronger condition that S can be represented as a sum of squares of other polynomials. Precisely, let $\mathbb{R}[\mathbf{a}]_{N,2d}$ denote the set of degree- $2d$ polynomials in $\mathbf{a} \in \mathbb{R}^N$, and let $\Sigma[\mathbf{a}]_{N,2d}$ denote its subset of sum-of-squares (SOS) polynomials,

$$\Sigma[\mathbf{a}]_{N,2d} := \left\{ p \in \mathbb{R}[\mathbf{a}]_{N,2d} : \exists k \in \mathbb{N}, q_1, \dots, q_k \in \mathbb{R}[\mathbf{a}]_{N,d} \text{ such that } p(\mathbf{a}) = \sum_{i=1}^k q_i(\mathbf{a})^2 \right\}. \quad (24)$$

We enforce $S(\mathbf{a}) \geq 0$ by requiring $S \in \Sigma[\mathbf{a}]_{N,2d}$. The degree of V can be no larger than that of S and may need to be smaller, so it suffices to choose V from $\mathbb{R}[\mathbf{a}]_{N,2d}$. With the degree of S no greater than $2d$, the best bound that can be proved using the SOS framework is

$$\bar{\Phi}_N \leq B_{N,2d} := \min_V B \quad \text{s.t.} \quad V \in \mathbb{R}[\mathbf{a}]_{N,2d}, \\ S \in \Sigma[\mathbf{a}]_{N,2d}. \quad (25)$$

The tunable parameters are the coefficients in V , which appear linearly in V and S , and the bound B , which appears linearly in S . Thus the SOS constraint is convex, and the minimization problem can be formulated as an SDP and solved computationally [47].

The bounds on truncated averages $\bar{\Phi}_N$ found by solving (25) are not necessarily bounds on $\bar{\Phi}$ in the full PDE, so we consider the limit of these bounds:

$$B_{2d} := \limsup_{N \rightarrow \infty} B_{N,2d}. \quad (26)$$

The bound $\bar{\Phi} \leq B_{2d}$ holds for the PDE if for every PDE solutions $u(x,t)$ there exists a sequence of solutions to truncated systems where $\bar{\Phi}_N$ converges to $\bar{\Phi}$. This appears to be true for $\bar{\mathcal{E}}$ in the KSE, but we do not prove it here. In such cases, the PDE bound B_{2d} can be approximated by increasing N until $B_{N,2d}$ converges numerically, much like choosing spatial resolution when numerically integrating PDEs. In the computations for the KSE reported here the numerical values of $B_{N,2d}$ converge quickly. Nonetheless, since one obtains only numerical approximations of B_{2d} , these values are not guaranteed to be valid bounds for the PDE. For many purposes this is not important, and the approach described above would be practical. For other purposes, such as computer-assisted proofs, it would be preferable to obtain bounds for the full PDE at finite N . This motivates the alternative framework of the following subsection, where the deviation between the truncated system (22) and the full PDE (6) is estimated rigorously.

2.4.2 Bounds for the full PDE

To construct an auxiliary functional for the full PDE (6) we cannot simply truncate the Galerkin expansion (20) after N terms. Instead we retain the “tail” $v(x,t)$ of the expansion,

$$u(x,t) = \sum_{n=1}^N a_n(t)u_n(x) + v(x,t). \quad (27)$$

Largely following the ideas of Goulart and Chernyshenko [20], we let the polynomial V depend not only on \mathbf{a} but also on $\mathbf{b} = (b_1, \dots, b_M)$, where each functional $b_m(v(\cdot, t))$ depends only on the tail. Assume the functionals included in \mathbf{b} allow $\Phi(u)$ to be represented exactly as $\Phi(\mathbf{a}, \mathbf{b})$. Expressions for the evolution of \mathbf{a} and \mathbf{b} can be derived from the PDE in the

general form

$$\frac{d}{dt}\mathbf{a} = \mathbf{f}(\mathbf{a}) + \mathbf{G}(\mathbf{a}, v), \quad (28)$$

$$\frac{d}{dt}\mathbf{b} = \mathbf{H}(\mathbf{a}, v), \quad (29)$$

where $\mathbf{f}(\mathbf{a})$ is the dynamics of the ODE truncation (22). The functional S whose nonnegativity would prove $\bar{\Phi} \leq B$ is then

$$S(u) = B - \Phi(\mathbf{a}, \mathbf{b}) - \mathbf{f}(\mathbf{a}) \cdot \nabla_{\mathbf{a}} V(\mathbf{a}, \mathbf{b}) - [\mathbf{G}(\mathbf{a}, v) \cdot \nabla_{\mathbf{a}} V(\mathbf{a}, \mathbf{b}) + \mathbf{H}(\mathbf{a}, v) \cdot \nabla_{\mathbf{b}} V(\mathbf{a}, \mathbf{b})] \quad (30)$$

The expression inside the square brackets need not be determined by (\mathbf{a}, \mathbf{b}) alone since it can depend more generally on the tail v . Likewise equations (28)–(29) may not fully determine the evolution of (\mathbf{a}, \mathbf{b}) , in which case they form an “uncertain system” [20]. However, by estimating the bracketed expression analytically in terms of (\mathbf{a}, \mathbf{b}) , possibly with the help of SOS polynomial constraints, one can seek a polynomial $T(\mathbf{a}, \mathbf{b})$ such that $S(u) \geq T(\mathbf{a}, \mathbf{b})$ for all $u \in \mathcal{U}$. Then the bounding condition $S(u) \geq 0$ can be replaced by the stronger condition that $T(\mathbf{a}, \mathbf{b})$ is an SOS polynomial, and the optimization over $V(\mathbf{a}, \mathbf{b})$ can be formulated as an SDP. This approach is illustrated for the KSE in §2.5.2, where the only functional needed in \mathbf{b} is the energy of v .

2.5 Higher-degree auxiliary functionals for the KSE

Polynomial auxiliary functionals for the KSE have many degrees of freedom in their lower-order terms, but their leading terms are highly constrained. Proposition 1 proved in Appendix A implies that because \mathcal{E}_∞ is finite on all trajectories and $\mathcal{E}(u)$ is bounded below, an upper bound on $\bar{\mathcal{E}}$ can be proved only using functionals $V(u)$ that are bounded below. (The Proposition assumes that $\mathcal{E} < \infty$ implies $|V| < \infty$, but this is always true in finite truncations if $V(\mathbf{a})$ is continuous.) Since V and D_V must be bounded below and above, respectively, the leading terms of both functionals must be of even degree. Thus we constrain the leading term of V as in

$$V(u) = c \left(\int u^2 dx \right)^d + P(a_1, a_2, \dots), \quad (31)$$

where $d \geq 1$ is an integer and P is a polynomial of degree at most $2d - 1$. The leading term of V is conserved by the nonlinearity of the KSE, so D_V has a leading term of degree $2d$, rather than $2d + 1$. There exist other degree- $2d$ expressions that are conserved by the nonlinearity, such as $\int u^{2d} dx$, but we have obtained finite bounds only with the leading term in (31). Similarly, the non-quadratic Lyapunov functionals constructed for the Navier–Stokes equations in [25] have powers of the energy as their leading terms.

Since u is odd and periodic we use the orthonormal sine basis,

$$u_n(x) = (\pi L)^{-1/2} \sin(nx/L), \quad (32)$$

for the Galerkin expansion (20). The projections $a_n(t)$ are Fourier coefficients of $u(x, t)$, up to rescaling by $\sqrt{\pi L}$. We let P in (31) depend on the first N projections, and possibly on the energy of the tail also. All V defined in this way remain bounded along solutions of the KSE, as required.

2.5.1 Truncated systems

In the sine basis, the N -mode Galerkin truncation (22) of the KSE is [44]

$$f_n(\mathbf{a}) = \left(\frac{n}{L}\right)^2 \left[1 - \left(\frac{n}{L}\right)^2\right] a_n + \frac{1}{\sqrt{\pi L}} \frac{n}{L} \left[\frac{1}{2} \sum_{m=1}^{N-n} a_m a_{m+n} - \frac{1}{4} \sum_{m=1}^{n-1} a_m a_{n-m} \right]. \quad (33)$$

If bounds are to be computed only for truncated systems, many other bases could be chosen, although it would be more work to derive $f_n(\mathbf{a})$. To compute bounds for the full PDE as described in the next subsection, the sine basis has additional advantages due to each $u_n(x)$ being an eigenfunction of the KSE's linear operator.

The truncation of spatially averaged energy is $\mathcal{E}_N = \frac{1}{2\pi L} |\mathbf{a}|^2$, and the truncation of the auxiliary functional (31) is

$$V(\mathbf{a}) = c|\mathbf{a}|^{2d} + P(\mathbf{a}). \quad (34)$$

The polynomial $P(\mathbf{a})$ in N variables has degree $2d - 1$ or less. That is, $P \in \mathbb{R}[\mathbf{a}]_{N,2d-1}$. The best bound that can be proved using the optimization (25) with $V(\mathbf{a})$ of degree $2d$ is

$$\begin{aligned} \bar{\mathcal{E}}_N \leq B_{N,2d} := \min_{c,P} B \quad \text{s.t.} \quad & c \in \mathbb{R}, \\ & P \in \mathbb{R}[\mathbf{a}]_{N,2d-1}, \\ & S \in \Sigma[\mathbf{a}]_{N,2d}, \end{aligned} \quad (35)$$

where S is defined as in (23) with $\mathbf{f}(\mathbf{a})$ given by (33). We approximate bounds for the full KSE using these $B_{N,2d}$ by increasing N to approach the large- N limit B_{2d} defined in (26). In the case of quadratic V , the limit B_2 is the optimal bound (18) provable by the background method, and the coefficients of the linear function $P(\mathbf{a})$ are proportional to the Fourier coefficients of the background function $\zeta(x)$ as described in Appendix C. Increasing the polynomial degree $2d$ can only improve bounds or leave them unchanged. Here we have computed numerical approximations to B_{2d} over a range of domain sizes L for auxiliary functionals of degree $2d = 2, 4$, and 6 .

2.5.2 Full KSE

To bound energy in the KSE using the framework of §2.4.2, it suffices to let the auxiliary functional (31) depend on the first N sine mode amplitudes, $\mathbf{a} = (a_1, \dots, a_N)$, and the energy of the tail,¹

$$q^2(t) := \int v(x, t)^2 dx = \sum_{n=N+1}^{\infty} a_n(t)^2. \quad (36)$$

¹Here q^2 is twice as large as the quantity of the same name in [20].

Such V take the form

$$V(\mathbf{a}, q^2) = c(|\mathbf{a}|^2 + q^2)^d + P(\mathbf{a}, q^2), \quad (37)$$

where P is a polynomial in the $N + 1$ variables (\mathbf{a}, q) whose degree is no larger than $2d - 1$. That is, $P \in \mathbb{R}[\mathbf{a}, q]_{N+1, 2d-1}$. The uncertain system (28)–(29) takes a particular form that arises also in the study of the Navier–Stokes equations [20]:

$$\frac{d}{dt}\mathbf{a} = \mathbf{f}(\mathbf{a}) + \boldsymbol{\Theta}(\mathbf{a}, v), \quad (38)$$

$$\frac{d}{dt}\left(\frac{1}{2}q^2\right) = -\mathbf{a} \cdot \boldsymbol{\Theta}(\mathbf{a}, v) + \Gamma(v), \quad (39)$$

where here $\mathbf{f}(\mathbf{a})$ is given by (33) and

$$\Gamma(v) = \int v(-v_{xx} - v_{xxxx})dx, \quad (40)$$

$$\Theta_n(\mathbf{a}, v) = \frac{n}{2\pi^{1/2}L^{3/2}} \sum_{m=N-n+1}^{\infty} a_m a_{m+n}. \quad (41)$$

The functional (8) that must be nonnegative is therefore

$$S(u) = B - \mathcal{E} - \mathbf{f} \cdot \nabla_{\mathbf{a}} V - \boldsymbol{\Theta} \cdot \mathbf{M} - 2\frac{\partial V}{\partial q^2}\Gamma, \quad (42)$$

where

$$\mathbf{M}(\mathbf{a}, q^2) = \nabla_{\mathbf{a}} V - 2\frac{\partial V}{\partial q^2}\mathbf{a} = \nabla_{\mathbf{a}} P - 2\frac{\partial P}{\partial q^2}\mathbf{a}. \quad (43)$$

Although Γ and $\boldsymbol{\Theta}$ depend on the tail v , we can bound them analytically in terms of only (\mathbf{a}, q^2) . This lets us derive a lower bound $S(u) \geq T(\mathbf{a}, q^2)$, where T is a polynomial.

It is simple to estimate Γ in terms of q^2 since the sine basis is the eigenbasis of the linear operator $-(\partial_x^2 + \partial_x^4)$. The corresponding eigenvalues are $\lambda_n = (n/L)^2 - (n/L)^4$, so

$$\Gamma(v) \leq \lambda_{N+1}q^2. \quad (44)$$

Here we always choose $N > L$, in which case $\lambda_{N+1} < 0$. In order for the above estimate to produce a lower bound on the last term in (42), we require that $\frac{\partial V}{\partial q^2} \geq 0$ also. It is a convenient feature of the KSE that the Galerkin basis enabling the estimate (44) is the sine basis. In the case of the Navier–Stokes equations, obtaining an estimate analogous to (44) requires using the eigenbasis of the energy stability operator [20], which often must be computed numerically.

To estimate $\Theta \cdot \mathbf{M}$ in (42) we apply the triangle inequality, $|\Theta \cdot \mathbf{M}| \leq \sum_{n=1}^N |\Theta_n| |M_n|$, and then bound each $|\Theta_n|$ using the Cauchy–Schwarz inequality,

$$\begin{aligned} |\Theta_n| &\leq \frac{n}{2\pi^{1/2}L^{3/2}} \left(\sum_{m=N+1}^{\infty} a_m^2 \right)^{1/2} \left(\sum_{m=N-n+1}^{\infty} a_m^2 \right)^{1/2} \\ &\leq \frac{n}{2\pi^{1/2}L^{3/2}} \left(q^2 + \sum_{m=N-n+1}^N a_m^2 \right). \end{aligned} \quad (45)$$

To eventually obtain a polynomial lower bound on $S(u)$, we must bound each $|M_n|$ by an expression without absolute values. For this we introduce polynomials $R_n(\mathbf{a}, q^2)$ and ensure that $|M_n| \leq R_n$ for all (\mathbf{a}, q^2) by requiring

$$-R_n(\mathbf{a}, q^2) \leq M_n(\mathbf{a}, q^2) \leq R_n(\mathbf{a}, q^2). \quad (46)$$

We find it suffices for R_n to have the same polynomial degree as M_n . The preceding approach to bounding $\Theta \cdot \mathbf{M}$ differs from that of [20], where the term analogous to $\Theta \cdot \mathbf{M}$ is bounded by $|\Theta \cdot \mathbf{M}| \leq \|\Theta\|_2 \|\mathbf{M}\|_2$, and then $\|\Theta\|_2$ is estimated. We have implemented both approaches for the KSE and find that using the sharper estimate (45) greatly improves the eventual bounds on $\bar{\mathcal{E}}$.

A lower bound on the $S(u)$ functional (42) follows from the above estimates on Γ , $|\Theta_n|$, and $|M_n|$. In particular, $S(u) \geq T(\mathbf{a}, q^2)$ with

$$\begin{aligned} T(\mathbf{a}, q^2) &= B - \frac{1}{2\pi L} (|\mathbf{a}|^2 + q^2) - \mathbf{f} \cdot \nabla_{\mathbf{a}} V - 2\lambda_{N+1} \frac{\partial V}{\partial q^2} \\ &\quad - \frac{1}{2\pi^{1/2}L^{3/2}} \sum_{n=1}^N n R_n \left(q^2 + \sum_{m=N-n+1}^N a_m^2 \right), \end{aligned} \quad (47)$$

provided that $\frac{\partial V}{\partial q^2} \geq 0$ and each R_n satisfies (46). Replacing each polynomial inequality with an SOS constraint gives:

$$T(\mathbf{a}, q^2) \in \Sigma[\mathbf{a}, q]_{N+1, 2d}, \quad (48)$$

$$\frac{\partial V}{\partial q^2}(\mathbf{a}, q^2) \in \Sigma[\mathbf{a}, q]_{N+1, 2d-2}, \quad (49)$$

$$R_n(\mathbf{a}, q^2) - M_n(\mathbf{a}, q^2) \in \Sigma[\mathbf{a}, q]_{N+1, 2d-2}, \quad \forall n \in \{1, \dots, N\}, \quad (50)$$

$$R_n(\mathbf{a}, q^2) + M_n(\mathbf{a}, q^2) \in \Sigma[\mathbf{a}, q]_{N+1, 2d-2}, \quad \forall n \in \{1, \dots, N\}. \quad (51)$$

The best bound that can be proved in this framework for S of degree no more than $2d$ is

$$\begin{aligned} \bar{\mathcal{E}} \leq B_{N, 2d}^{pde} &:= \min_{c, P} B \quad \text{s.t.} \quad c \in \mathbb{R}, \\ &\quad P \in \mathbb{R}[\mathbf{a}, q]_{N+1, 2d-1}, \\ &\quad (48) - (51). \end{aligned} \quad (52)$$

If $V(\mathbf{a}, q^2)$ proves $\bar{\mathcal{E}} \leq B_{N,2d}^{pde}$ for the full KSE in the above framework, $V(\mathbf{a}, 0)$ proves $\bar{\mathcal{E}}_N \leq B_{N,2d}$ in the truncated framework (35) for some $B_{N,2d} \leq B_{N,2d}^{pde}$. However, only the larger value $B_{N,2d}^{pde}$ is guaranteed to be a bound for the full KSE at finite N . We have solved (52) computationally by converting it into an SDP. Results are reported in §4 for degree-4 auxiliary functionals over a range of domain sizes L . The resulting bounds converge from above as $N \rightarrow \infty$.

3 Steady states of the KSE and its truncations

In order to judge the quality of the bounds reported in the next section, let us review the simplest odd steady states of the KSE [21]. The zero state $u = 0$ is globally attracting when $L < 1$. As the domain size increases through $L = 1$, the zero state becomes linearly unstable, and a pitchfork bifurcation gives rise to a pair of nonlinear steady equilibria that we call E_1 . The pair of states are mapped to one another by $u \mapsto -u$ and so have the same energy. The mean energy along the E_1 branch is shown in the bifurcation diagram of figure 1(a), and $u(x)$ on the E_1 branch is plotted in figure 1(b-d) for three different domain sizes. Rescaled versions of the bifurcation at $L = 1$ occur at all integer values of L . This can be anticipated because for any solution of the KSE in a domain of size $2\pi L$, taking n periods of this solution gives a solution in a domain of size $2\pi Ln$. Thus for all positive integers n there exist branches of “primary equilibria” E_n where $u_{E_n}(x) = u_{E_1}(x/n)$. Figure 1(a) shows these E_n branches, along with other equilibria that we computed by applying the bifurcation analysis software MatCont [11] to the Galerkin truncation (33) with $N = 32$. Many of the bounds on $\bar{\mathcal{E}}$ reported in the next section are approximately equal to the upper envelope of the E_n curves in figure 1(a). In such cases we can conclude that the bounds are sharp and are saturated by one of the primary equilibria.

The bifurcation structure of Galerkin truncations of the KSE informs the number of modes that we must include in our bounding computations. With N fixed, the deviation of the ODE system from the full PDE worsens as L is raised. In the PDE, each E_n state is n exact copies of the E_1 state. In a truncation with fixed N , the branches become more under-resolved as n increases; the spectral content of the E_n branch is every n^{th} sine mode, so each E_n is approximated by no more than N/n modes. This under-resolution causes the ODE system to be unbounded when $L \geq N/2 + 1$ because every E_n branch for $n \in [N/2 + 1, N]$ is truncated after only the single mode u_n , and the linear instability of the u_n mode does not saturate without the u_{2n} mode. For a given L , finite bounds are possible for the truncated system or the full KSE only if $N \geq 2L - 2$.

4 Bounds on time-averaged energy

We have computed upper bounds on $\bar{\mathcal{E}}$ both for large Galerkin truncations of the KSE and for the full KSE by solving the SOS optimization problems (35) and (52), respectively.

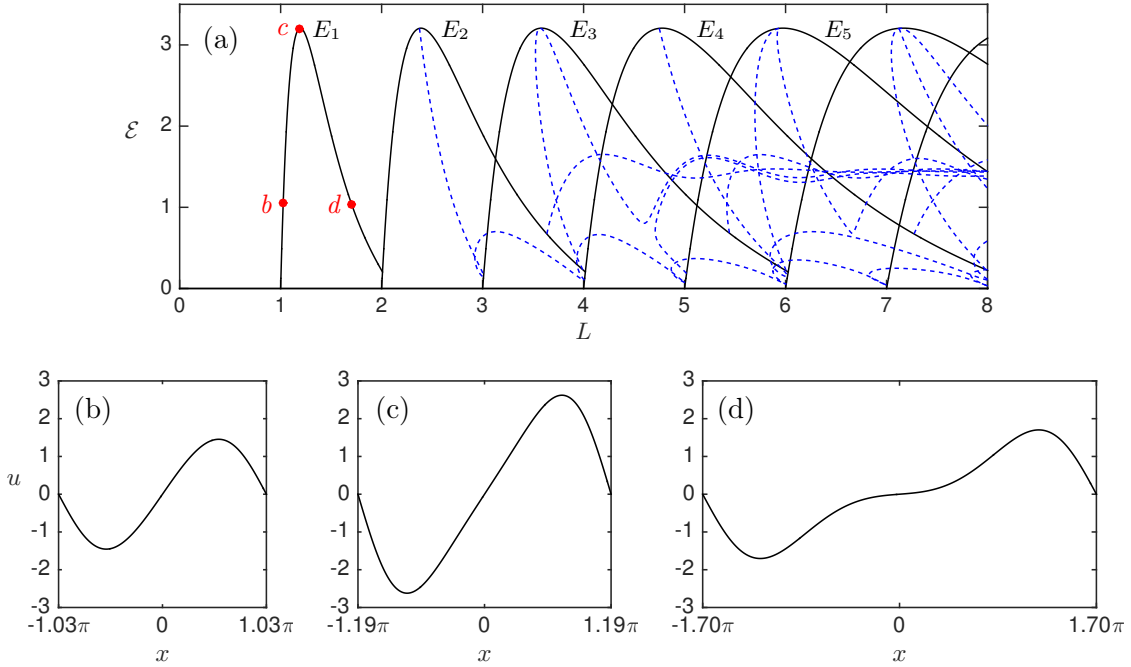


Figure 1: (a) Bifurcation diagram showing the spatially averaged energy \mathcal{E} of primary equilibria E_n (—) and odd secondary equilibria (---) of the KSE. Stability of equilibria is not indicated. (b-d) Steady solutions $u(x)$ on the E_1 branch at the three points indicated (●) in panel (a), where the values of L are (b) 1.03 , (c) 1.19 , and (d) 1.70 .

The software YALMIP [32, 33] was used to reformulate the SOS problems as SDPs and interface with SDP solvers. When possible we used the solver Mosek [36]. As SDPs grew in size because of increasing polynomial degree or number of modes, the memory footprint of Mosek became prohibitive (e.g., well over 128 GB). For these large SDPs we used the solver SCS [40, 41], whose first-order method converges to a given precision much more slowly than Mosek’s interior-point method but requires less memory. Appendix B details our computational implementation, including convergence criteria.

For an example of how bounds converge as the number of modes N increases, consider the KSE in a domain with $L = 3.5$. At this L , the E_3 branch has the largest mean energy among all equilibria shown in figure 1(a). For each N between 6 and 18, table 1 reports \mathcal{E}_{E_3} in the truncated system, as well as bounds for the truncated system and for the full PDE that we computed using both quadratic and quartic auxiliary functionals. The value of \mathcal{E}_{E_3} converges quickly and is accurate to 7 digits in the 12-mode system, wherein the E_3 branch is resolved by 4 nonzero modes. In the case of quadratic V , the truncated bounds $B_{N,2}$

Table 1: Upper bounds on mean energy for odd solutions of the KSE in a domain of size $2\pi L = 7\pi$, computed using quadratic and quartic V . Values tabulated for various numbers of modes (N) are the energy of the third primary equilibrium (\mathcal{E}_{E_3}) in the truncated system, bounds on mean energy in the truncated system ($B_{N,2d}$) computed using (35), and bounds on mean energy in the full PDE ($B_{N,2d}^{pde}$) computed using (52). To the tabulated precision, $\mathcal{E}_{E_n} = B_{N,4}$ for each N .

N	\mathcal{E}_{E_3}	quadratic V		quartic V	
		$B_{N,2}$	$B_{N,2}^{pde}$	$B_{N,4}$	$B_{N,4}^{pde}$
6	3.126 656	9.074 245	12.291 86	3.126 656	
7	"	9.929 391	9.288 534	"	
8	"	8.767 367	9.114 863	"	
9	3.173 413	9.013 554	9.028 150	3.173 413	12.370 65
10	"	8.986 130	9.009 991	"	3.546 301
11	"	9.002 760	9.004 201	"	3.451 817
12	3.174 051	9.002 593	9.003 712	3.174 051	3.177 370
13	"	9.003 391	9.003 431	"	3.176 181
14	"	9.003 369	9.003 420	"	3.176 139
15	"	9.003 411	9.003 410	"	3.174 076
16	"	9.003 408	9.003 410	"	3.174 071
17	"	9.003 410	9.003 409	"	3.174 068
18	"	9.003 409	9.003 409	"	3.174 054

and PDE bounds $B_{N,2}^{pde}$ both converge toward the optimal bound (18) of the background method, which is not a sharp bound on $\bar{\mathcal{E}}$ at this L . In the case of quartic V , on the other hand, $B_{N,4}$ and $B_{N,4}^{pde}$ both converge to \mathcal{E}_{E_3} up to 6 digits. This suggests that the E_3 state maximizes $\bar{\mathcal{E}}$ among odd solutions of the KSE at $L = 3.5$, and that a quartic V provides the sharp bound.

It is better to compute $B_{N,2d}$, as opposed to $B_{N,2d}^{pde}$, when one's objective is to approximate the large- N limit, thereby approximating the best bound provable within some infinite-dimensional class \mathcal{V} of auxiliary functionals. This is because $B_{N,2d}$ is less expensive to compute at each N (cf. Appendix A) and often converges faster as $N \rightarrow \infty$, as in the quartic- V bounds of table 1. We have computed such results up to the largest domain sizes in which it was tractable to approximate the large- N limit. Section 4.1 reports these findings.

On the other hand, one must compute $B_{N,2d}^{pde}$, as opposed to $B_{N,2d}$, when one's objective is to obtain rigorous bounds for the PDE. The exact value of $B_{N,2d}^{pde}$ at any finite N constitutes such a bound. Full rigor requires also accounting for error in the formulation of the SOS program as an SDP, and in the numerical solution of the SDP itself. This can be done with interval arithmetic using the software VSDP [28], as illustrated in [17]. In the

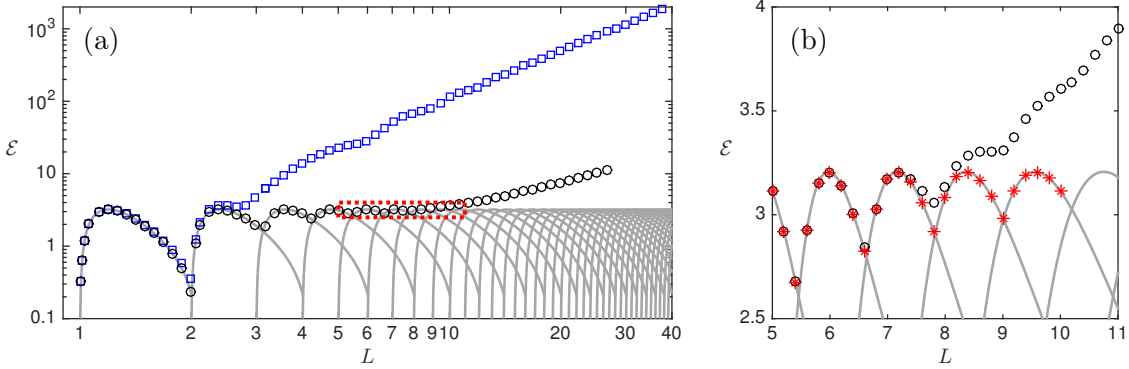


Figure 2: Upper bounds on the mean energy of odd solutions, computed for large truncations of the KSE using auxiliary functionals of degree 2 (□), 4 (○), and 6 (*). Mean energies of primary equilibria are shown also (—). Degree-6 bounds are shown only in panel (b), which is a detailed view of the boxed region in panel (a).

present work we simply approximate $B_{N,2d}^{pde}$ numerically as a proof of concept for the PDE bounding framework of §2.5.2. Section 4.2 reports these findings.

4.1 Bounds for ODE truncations

We have computed bounds $\bar{\mathcal{E}} \leq B_{N,2d}$ for the truncated KSE by solving (35) using truncated auxiliary functionals $V(\mathbf{a})$ of polynomial degrees 2, 4, and 6. To approximate the large- N limit at a given value of L , we determined the primary equilibrium E_n with the largest mean energy and then used the criterion $N \geq 3n$. In computationally easier cases, including all bounds with quadratic V , we included many more than $3n$ modes. Results in these over-resolved cases suggest that the $N \geq 3n$ criterion gives values of $B_{N,2d}$ within 1% of the large- N limit, B_{2d} , as reflected in the example of table 1 where the criterion requires $N \geq 9$. Bounds were computed with quadratic V for $L \leq 100$, with quartic V for $L \leq 26.6$, and with sextic V for $L \leq 10$.

Bounds on $\bar{\mathcal{E}}$ for various L , computed using quadratic and quartic V , are plotted in figure 2(a). Energies \mathcal{E}_{E_n} of the KSE’s primary equilibria are plotted also for comparison. A region of this plot is expanded in figure 2(b), which shows bounds computed using quartic and sextic V . When a bound is saturated by one of the E_n branches (up to numerical error) we conclude that it is sharp.

The polynomial degree of V is evidently very important. Quadratic V give sharp bounds (to within 1%) only for $L \lesssim 1.25$, whereas quartic V give sharp bounds for $L \lesssim 7.5$. Sextic V give sharp bounds up to the largest domain ($L = 10$) in which we computed them. We suspect that V of any fixed polynomial degree $2d$ can give sharp bounds on $\bar{\mathcal{E}}$ only up to some finite domain size. This suggests that non-polynomial V may be needed to prove

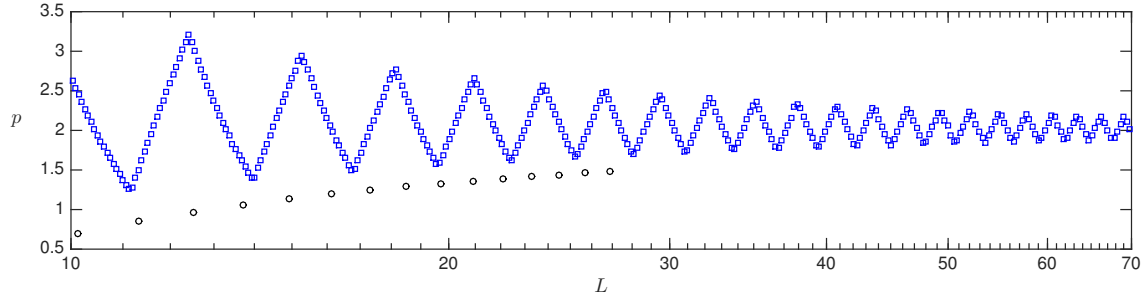


Figure 3: Local exponents of power laws cL^p fit to upper bounds on mean energy for auxiliary functionals of degree 2 (□) and 4 (○). The bound values are shown in figure 2(a) over a different range of L .

optimal bounds in the $L \gg 1$ limit.

Even if higher-degree polynomial V cannot produce $O(1)$ bounds when $L \gg 1$, they might yield bounds that scale better than those proved using quadratic V . Our quadratic- V bounds, which are tantamount to the optimal background method, are fit well by $B_2 \sim 1.12 L^2$ over $40 \leq L \leq 100$. Appendix C gives examples of the corresponding background functions $\zeta(x)$. The fact that $\bar{\mathcal{E}} \leq O(L^2)$ follows from the result $\mathcal{E}_\infty \leq O(L^2)$ proved using the background method [3]. Apparently bounding $\bar{\mathcal{E}}$ directly by the background method cannot improve this scaling, although our prefactor is smaller by several orders of magnitude. The quartic- V bounds in figure 2 have not reached the asymptotic regime, but we can discern a trend by examining their local slope.

After refining the results of figure 2(a) by computing bounds at many more values of L , we have fit local power laws of the form cL^p . That is, we approximate the exponent p by a local linear fit of $\log B_{2d}$ to $\log L$. Figure 3 shows how p varies with L for quadratic and quartic V . In the quadratic case, the optimal bounds have a local exponent that oscillates while converging to 2. The oscillations have a period of approximately 2.8 with no obvious connection to the KSE's bifurcation structure; they might correspond to bifurcations in the Euler–Lagrange equations governing the optimal background function $\zeta(x)$ in (18). In the case of quartic V , on the other hand, bounds oscillate mildly with a shorter period that reflects the shape of the envelope of the E_n energies, as can be seen in figure 2(b). This oscillation is not evident in figure 3 because, to make the trend clearer, we have estimated p using quartic- V bounds computed only at values of L where the envelope of E_n energies has a local maximum. That is, we include bounds computed at $L = 1.1947 n$ for $8 \leq n \leq 23$. The limit of p is apparently larger than $2/3$, meaning that when $L \gg 1$ the quartic- V bounds will not be as good as the $O(L^{2/3+})$ bounds proved by entropy methods [16, 42]. It remains unclear whether the limit of p for quartic- V bounds is less than 2, which would indicate an improvement upon the $O(L^2)$ scaling of quadratic- V bounds.

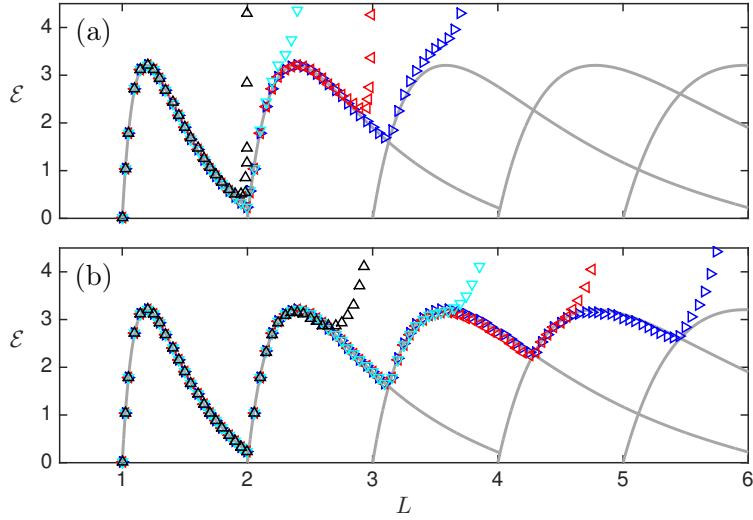


Figure 4: Upper bounds on mean energy computed using quartic V for (a) the full KSE and (b) truncations of the KSE. The number of modes (N) used to compute the bounds are 4 (Δ), 6 (\triangledown), 8 (\triangleleft), and 10 (\triangleright). Mean energies of primary equilibria are shown also (—).

4.2 Bounds for the full PDE

We have computed bounds $\bar{\mathcal{E}} \leq B_{N,4}^{pde}$ for the KSE by solving (52) for quartic auxiliary functionals $V(\mathbf{a}, q^2)$. These bounds cannot be sharp when $L \gtrsim 7.5$ since they cannot be better than the quartic- V bounds for the truncated system shown in figure 2(b), but we find they can be sharp at smaller L .

Figure 4(a) shows bounds $B_{N,4}^{pde}$ computed for various L using $N = 4, 6, 8$, and 10 modes. Every plotted point is a valid bound for the PDE, or at least it would be if the SDP producing it were solved to infinite precision. Bounds are very good for small domains and then quickly blow up as L increases. When more modes are included, this blowup is postponed until larger L . For each N , the bounds $B_{N,4}^{pde}$ blow up at smaller L than the corresponding bounds $B_{N,4}$ for the truncated system, which are shown in figure 4(b). The latter blow up as $L \rightarrow N/2 + 1$, which is when the N -mode truncated system becomes unbounded (cf. §3). Unlike the PDE bounds in figure 4(a), some $B_{N,4}$ values plotted in figure 4(b) are *not* valid bounds for the PDE—they lie slightly below the E_n curves. This occurs because under-resolved E_n states in truncations of the KSE have slightly less mean energy than in the full KSE.

Figure 5 shows sharp bounds on $\bar{\mathcal{E}}$ that we have computed for the KSE by solving (52). The number of modes included in the auxiliary functional (37) to produce bounds saturated by the E_1, E_2, E_3 , and E_4 branches were 6, 12, 18, and 24, respectively. Rigorous versions of these results could be computed using interval arithmetic as in [17]. Such bounds would

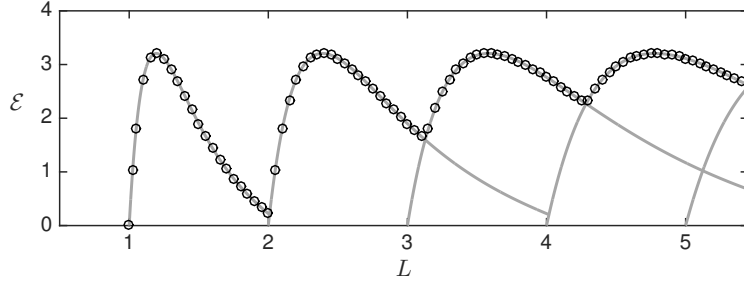


Figure 5: Upper bounds on $\bar{\mathcal{E}}$ for the KSE computed by solving (52) with quartic V . The bounds saturated by each of the first four branches of E_n equilibria (—) were computed using $N = 6n$ modes.

not be exactly sharp since interval arithmetic is inherently conservative, but we suspect they would be very close to sharp.

5 Conjectures and conclusions

We have illustrated methods for bounding time averages in nonlinear PDEs by constructing polynomial auxiliary functionals. This is a generalization of the background method, which is tantamount to using a subset of quadratic auxiliary functionals. Polynomial auxiliary functionals and the resulting bounds can be constructed with computer assistance. This is done by formulating sufficient conditions as polynomial optimization problems subject to sum-of-squares constraints, translating these problems into semidefinite programs, and solving the latter computationally. Two related approaches have been presented, both of which involve approximating the PDE by a system of ODEs derived by Galerkin truncation. The first is to compute bounds for the ODE systems using existing methods [5, 12, 17] and raise the truncation order until bounds converge. The limit is a bound for the PDE, provided that all PDE solutions are limits of solutions of truncated systems. The second approach is similar but also incorporates analytical estimates on the deviation between the PDE and its truncations. This produces bounds applying to the full PDE, despite the truncations being finite.

We have applied these methods to the Kuramoto–Sivashinsky equation, computing upper bounds on the spatiotemporally averaged energy $\bar{\mathcal{E}}$ of odd solutions for a variety of domain sizes $2\pi L$. Using the first approach where bounds are computed for large ODE truncations, we have obtained bounds using auxiliary functionals V of degree 2, 4, and 6. For each domain size, the number of modes was increased until the bounds converged. For V of fixed degree, bounds appear sharp for domains up to a certain size, beyond which they become increasingly conservative as L grows. Quadratic V give sharp bounds (to within 1%) only for $L \lesssim 1.25$, while quartic V give sharp bounds for $L \lesssim 7.5$, and sextic V give

sharp bounds on the entire range $L \leq 10$ that was computationally accessible. The reason sharp bounds can be identified as such is that they are saturated (up to numerical error) by one of the primary equilibria, E_n , each of which is simply n copies of the first nonzero equilibrium.

To demonstrate the second approach, where bounds for the full PDE are produced by augmenting ODE truncations with analytical estimates, we used quartic V to compute sharp bounds on $\bar{\mathcal{E}}$ for $L \lesssim 5.5$. This approach is more computationally expensive and may not be applicable to as broad a range of nonlinear PDEs, but it is merited when one seeks results that are rigorous to the standard of a computer-assisted proof. This could be accomplished by augmenting SDP computations with interval arithmetic as in [17].

Our findings bear on the conjecture that solutions of the KSE obey $\bar{\mathcal{E}} \leq O(1)$ for $L \gg 1$. The sharp bounds we computed for $L \leq 10$ suggest the following stronger conjecture.

Conjecture 1. *For all odd solutions $u(x, t)$ of the KSE (1) and $L > 1$,*

$$\max_{u(x,t)} \bar{\mathcal{E}} = \max_n \mathcal{E}_{E_n}. \quad (53)$$

As $L \rightarrow \infty$ the righthand maximum is achieved by periodic copies of the E_1 state with the largest mean energy—the equilibrium with spatial period $2\pi L \approx 7.48$ that is shown in figure 1(c). Conjecture 1 could be strengthened in two ways: by not restricting $u(x, t)$ to the odd subspace, and by replacing the time average $\bar{\mathcal{E}}$ with \mathcal{E}_∞ , the largest instantaneous energy on the attractor. We are not aware of counterexamples to these stronger conjectures; the computational results in figures 14 and 15 of [9] are consistent with them. However, our bounds give positive evidence only for the weaker conjecture stated above, and only for $L \leq 10$. Regarding the use of auxiliary functionals to prove Conjecture 1, our findings suggest another conjecture.

Conjecture 2. *(a) For odd solutions $u(x, t)$ of the KSE (1) and any fixed L , there exists an auxiliary functional V of finite polynomial degree $2d \in 2\mathbb{N}$ that can be used to prove Conjecture 1. In particular, as the truncation order N approaches infinity, bounds on $\bar{\mathcal{E}}$ for the truncated system given by (35) and bounds for the full PDE given by (52) satisfy, respectively,*

$$\lim_{N \rightarrow \infty} B_{N,2d} = \max_n \mathcal{E}_{E_n}, \quad \lim_{N \rightarrow \infty} B_{N,2d}^{pde} = \max_n \mathcal{E}_{E_n}. \quad (54)$$

(b) However, satisfying (54) as $L \rightarrow \infty$ requires $2d \rightarrow \infty$, meaning that V of fixed polynomial degree cannot provide sharp bounds in the large-domain limit.

The L -dependence of our bounds hints at what type of auxiliary functionals might be used to prove analytically that $\bar{\mathcal{E}} \leq O(1)$. Apparently the best bounds provable using quadratic V are $\bar{\mathcal{E}} \leq O(L^2)$. Increasing the polynomial degree of V improves bounds on $\bar{\mathcal{E}}$ at fixed L , but it is unclear whether V of any fixed degree can give bounds growing

more slowly than $O(L^2)$ when $L \gg 1$. As asserted by Conjecture 2, it seems that sharp bounds require the degree of V to continue growing as $L \rightarrow \infty$. This suggests that to seek $O(1)$ bounds analytically in this limit, one should consider auxiliary functionals with non-polynomial dependence on u .

Beyond the KSE, the background method has been used to bound time averages in physical systems governed by the Navier–Stokes equations and other nonlinear PDEs. In many cases this produces bounds on time averages that are not sharp. Our findings for the KSE suggest that many such results of the background method could be sharpened by generalizing auxiliary functionals beyond the simplest quadratic case. This can be done analytically or computationally. Here we have demonstrated computational approaches that can give sharp bounds, although only when the intrinsic dimension of the dynamics is low enough for the computations to be tractable.

Pushing our SDP-based methods to higher-dimensional regimes requires overcoming the relatively poor scalability of algorithms for solving SDPs. In this work we tackled fairly large SDPs by using a solver that implements a first order algorithm, rather than an interior point algorithm, which reduces memory requirements but greatly increases computation time. A second option is to use more tractable relaxations of sum-of-squares constraints based on linear or second-order cone programming [1], and a third is to optimize directly over SOS polynomials without recourse to SDPs [45]. Algorithmic improvements may also be accompanied by restrictions to auxiliary functionals that yield polynomial optimization problems with a favorable sparse structure, to which sparse SOS conditions can be applied [31, 54]. It remains to be seen how much these techniques can improve upon bounds proved by the background method for a variety of PDEs. For the KSE, at least, our finding demonstrate that the improvement can be quite substantial.

Acknowledgements

During this work DG was partially supported by a James Van Loo Post-Doctoral Fellowship and NSF award DMS–1515161, and GF was partially supported by EPSRC studentship award 1864077. Both authors are grateful for the hospitality of the Geophysical Fluids Dynamics program at the Woods Hole Oceanographic Institution, where some of this work was carried out, and for very beneficial exchanges with Charles Doering, Ian Tobasco, and Andrew Wynn.

A Boundedness of auxiliary functionals

The following proposition is used in §2.5 to explain constraints on the leading term of auxiliary functionals for the KSE.

Proposition 1. *Suppose the PDE (6) is well-posed with solutions $u(x, t)$ remaining in a function space \mathcal{U} , meaning that $u(\cdot, t) \in \mathcal{U}$ for all $t \geq 0$. Suppose also that V proves a*

finite bound $\bar{\Phi} \leq B$ via the auxiliary functional condition $B - \Phi(u) - D_V(u) \geq 0$, and that $|\Phi(u)| < \infty$ implies $|V(u)| < \infty$. If Φ_∞ is finite for all PDE solutions $u(x, t)$, then $V(u)$ is bounded below for all $u \in \mathcal{U}$.

Proof. If Φ_∞ defined by (11) is finite there exists an absorbing set $\mathcal{A} = \{u \in \mathcal{U} : \Phi(u) \leq B_\infty\}$, and we can choose $B_\infty > B$ without loss of generality. Since Φ is uniformly bounded on \mathcal{A} , by assumption V is also, so $\inf_{\mathcal{A}} V(u)$ is finite. To show that V is bounded below on \mathcal{U} , it suffices to show $\inf_{\mathcal{U} \setminus \mathcal{A}} V(u) \geq \inf_{\mathcal{A}} V(u)$.

Let $u_0(x) \in \mathcal{U} \setminus \mathcal{A}$. Consider a PDE solution $u(x, t)$ with initial condition $u(x, 0) = u_0(x)$. There exists a finite first time T at which $\Phi(u(x, T)) = B_\infty$, prior to which $\Phi(u(x, t)) > B_\infty$. Recalling that $D_V(u(\cdot, t)) = \frac{d}{dt} V(u(\cdot, t))$ along all trajectories, we integrate the inequality $\frac{d}{dt} V(u(\cdot, t)) \leq B - \Phi(u(\cdot, t))$ up to time T to find

$$V(u(x, T)) - V(u_0(x)) \leq \int_0^T [B - \Phi(u(x, t))] dt \leq \int_0^T [B_\infty - \Phi(u(x, t))] dt. \quad (55)$$

The righthand integrand is nonpositive, so $V(u_0(x)) \geq V(u(x, T)) \geq \inf_{\mathcal{A}} V(u)$. This proves the claim that $V(u)$ is bound below uniformly for all $u \in \mathcal{U}$. \square

B Computational implementation

When using YALMIP to reformulate the SOS optimization problems (35) and (52) as SDPs, we decreased the size of the SDPs by imposing a particular symmetry on the auxiliary functionals. When solving (35), for instance, the lower-order part P did not include all possible monomials. A monomial, denoted by $a_{i_1} a_{i_2} \cdots a_{i_K}$ with possible repetition in the subscript values, was included in P only if the sum of its indices is even. For instance, V of quartic degree could contain the monomial $a_3^2 a_6$ (when $N \geq 6$) but not $a_1 a_2 a_4$. We imposed this symmetry on P to save computational cost after numerous solutions of (35) with general $P \in \mathbb{R}[\mathbf{a}]_{N, 2d-1}$ all returned optimal P with the symmetry. The interpretation of the symmetry is simple in the case of quadratic V , where it means that P contains only every second linear coefficient. This corresponds to a background function $\zeta(x)$ that is πL -periodic (cf. Appendix C). We have not proved analytically that optimal P must have this structure, but nonetheless bounds computed with restricted P are valid.

Although the expression (33) for the truncated system \mathbf{f} does not share the symmetry imposed on P , the expression $\mathbf{f} \cdot \nabla V$ does, and so does the polynomial S that is required to be SOS. The Gram matrix representation of S , which is central to the translation of SOS constraints into SDP constraints, inherits block diagonal structure from the symmetry of S [14, 33]. Ordinarily YALMIP can detect symmetries of S and block diagonalize its Gram matrix accordingly, but many of the problems solved here were too large for this functionality. Thus we modified YALMIP to impose the particular block diagonal structure arising in the present cases.

Table 2: Upper bounds on mean energy for odd solutions of the truncated KSE, computed using quartic auxiliary functionals ($2d = 4$). Tabulated values give the number of modes in the truncation (N), the domain size ($2\pi L$), the computed bound ($B_{N,2d}$), the SDP solver used, the number of iterations, the time of the SDP solution, and the memory required to set up and solve the SDP.

N	L	$B_{N,4}$	solver	steps	time	memory
12	3	1.900 280	Mosek	17	1 sec.	0.42 GB
		1.900 284	SCS	197 260	311	0.41
20	5	3.113 014	Mosek	17	59	0.85
		3.113 034	SCS	265 880	2 842	0.43
28	7	3.174 205	Mosek	32	2 659	5.12
		3.174 393	SCS	7 851 400	304 200	0.63

All SDP solutions were performed on a single core. The SDPs were solved by an interior-point algorithm using Mosek when the memory footprint to do so was not prohibitively large (e.g., larger than 128 GB). All bounds for the full KSE reported in §4.2 were computed using Mosek. Bounds for truncations of the KSE reported in §4.1 were computed using Mosek for all quadratic V , for quartic V when $N \leq 36$, and for sextic V when $N \leq 16$. Solver tolerances were set to 10^{-12} , resulting in many computations terminating when progress stalled. In the worst such cases, tolerances were still smaller than 10^{-7} . These tolerances alone do not give an error bound on the approximate optimum of the SDPs—that is, on $B_{N,2d}$ or $B_{N,2d}^{pde}$. This would require more sophisticated analysis, as implemented by the software VSDP [28]. However, the fact that various bounds are sharp to 5 or more digits (e.g., in table 1) suggests that values of $B_{N,2d}$ and $B_{N,2d}^{pde}$ computed using Mosek are at least this precise.

The first-order solver SCS was applied to SDPs too large for Mosek. Solver tolerances were set to 10^{-4} , and all solutions reached these tolerances. For the largest SDPs solved here, where V was quartic and N was larger than 50, meeting these tolerances required running SCS for over a month at each value of L . The formulation of these large SDPs using YALMIP took between a few hours and a day. Comparing SCS and Mosek solutions for smaller SDPs suggests that tolerances of 10^{-4} in SCS give approximate values of $B_{N,2d}$ that are precise to at least 4 digits. This can be seen in table 2, which shows examples of bounds computed with both solvers. The table also shows the number of iterations required for solutions to meet tolerances, the time of the SDP solver running with a single thread on a 2.5 GHz Intel Xeon processor, and the memory required to formulate the SDP using YALMIP and then run the solver. For the purposes of this table and the next one, all Mosek tolerances were 10^{-8} . Although times of different solvers cannot be directly compared, even when tolerances are nominally identical, it is clear that SCS converges more slowly than Mosek, and that its memory footprint grows more slowly with the problem size.

Table 3: Time required by Mosek to solve the SDP formulations of (35) and (52) with quartic auxiliary functionals to obtain bounds for the truncated KSE ($B_{N,4}$) and full KSE ($B_{N,4}^{pde}$), respectively, for various numbers of modes (N) and domain sizes ($2\pi L$).

N	L	Solving (35)		Solving (52)	
		$B_{N,4}$	time	$B_{N,4}^{pde}$	time
8	2	0.222 904	0.1 sec.	0.222 938	0.6 sec.
12	3	1.900 280	1.0	1.900 440	5.5
16	4	2.762 934	13.3	2.763 049	41.9

For a fixed number of modes, computing bounds for the truncated KSE by solving (35) is less expensive than computing bounds for the full KSE by solving (52). Table 3 gives some examples of the wall time required to solve the SDPs arising from (35) and (52), respectively, using Mosek with a single thread.

C Optimal background functionals

The bounds we have produced using quadratic auxiliary functionals can be translated into the language of the background method if desired. When $V(\mathbf{a})$ is quadratic, the optimization (35) of bounds for the truncated KSE is a truncated version of the background method optimization (18) in spectral space. So long as enough modes are included in the truncation, optimal quadratic $V(\mathbf{a})$ provide close approximations to the optimal coefficients α and background functions $\zeta(x)$ solving (18). The optimal V have only even-index a_n in their linear terms, so they take the form

$$V(\mathbf{a}) = c|\mathbf{a}|^2 + \sum_{n=1}^{\lfloor N/2 \rfloor} c_{2n} a_{2n}, \quad (56)$$

and the SDP solver returns optimal values of the coefficients c and c_{2n} . Meanwhile, after dropping the irrelevant term $\frac{\alpha}{2} \int \zeta^2 dx$, the auxiliary functional (16) defined using the background function can be expanded in terms of Fourier coefficients as

$$V(u) = \frac{\alpha}{4\pi L} |\mathbf{a}|^2 - \frac{\alpha}{2\pi L} \sum_{n=1}^{\infty} a_n z_n, \quad (57)$$

where

$$\zeta(x) = (\pi L)^{-1/2} \sum_{n=1}^{\infty} z_n \sin(nx/L). \quad (58)$$

When $u(x, t)$ and $\zeta(x)$ in the background method are truncated after N modes, expressions (56) and (57) can be equated to find

$$\alpha = 4\pi L c, \quad \zeta(x) = -\frac{1}{2c(\pi L)^{1/2}} \sum_{n=1}^{\lfloor N/2 \rfloor} c_{2n} \sin(2nx/L). \quad (59)$$

Figure 6 shows some optimal α and $\zeta(x)$ for the background method, recovered from our quadratic V according to (59). Panel (a) shows that, as L increases, the optimal leading coefficient α oscillates and decreases, perhaps asymptoting to 8. The oscillations in α coincide with the oscillations in the slope of upper bounds shown in figure 3, although only the former quantity appears to depend smoothly on L . Figure 6(b) shows the optimal background function for $L = 10^{1.3} \approx 19.95$, with both x and ζ normalized by the domain size $2\pi L$. The shape of ζ strongly resembles background functions that have been constructed in [3, 13] for the related task of bounding the instantaneous energy \mathcal{E}_∞ . For reasons explained in [13], the optimal ζ has a period of πL as opposed to $2\pi L$, although nearly optimal ζ with a period of $2\pi L$ can still produce bounds with the same $O(L^2)$ scaling [3]. The scaling of our optimal ζ as $L \rightarrow \infty$ is similar to that in [3, 13]. Outside the boundary layers the slope $\zeta'(x)$ approaches a constant, as can be seen in figure 6(c), which shows normalized ζ near the central boundary layer for three different domain sizes. The limiting slope appears to be $3/4$, as opposed to $9/4$ in the \mathcal{E}_∞ bounding problem [13]. The boundary layer thickness scales as $O(L^{-1/3})$. This can be seen by the collapse of profiles in figure 6(d), where the profiles in panel (c) are re-plotted with x normalized according to this scaling.

References

- [1] A. A. Ahmadi and A. Majumdar. DSOS and SDSOS optimization: LP and SOCP-based alternatives to sum of squares optimization. In *48th Annual Conference on Information Sciences and Systems*, pages 1–5, Princeton, USA, 2014. IEEE.
- [2] J. Anderson and A. Papachristodoulou. Advances in computational Lyapunov analysis using sum-of-squares programming. *Discret. Contin. Dyn. Syst. Ser. B*, 20:2361–2381, 2015.
- [3] J. C. Bronski and T. N. Gambill. Uncertainty estimates and L_2 bounds for the Kuramoto–Sivashinsky equation. *Nonlinearity*, 19:2023–2039, 2006.
- [4] S. Chernyshenko. Relationship between the methods of bounding time averages. *arXiv:1704.02475v2*, 2017.
- [5] S. I. Chernyshenko, P. Goulart, D. Huang, and A. Papachristodoulou. Polynomial sum of squares in fluid dynamics: a review with a look ahead. *Philos. Trans. R. Soc. A*, 372:20130350, 2014.

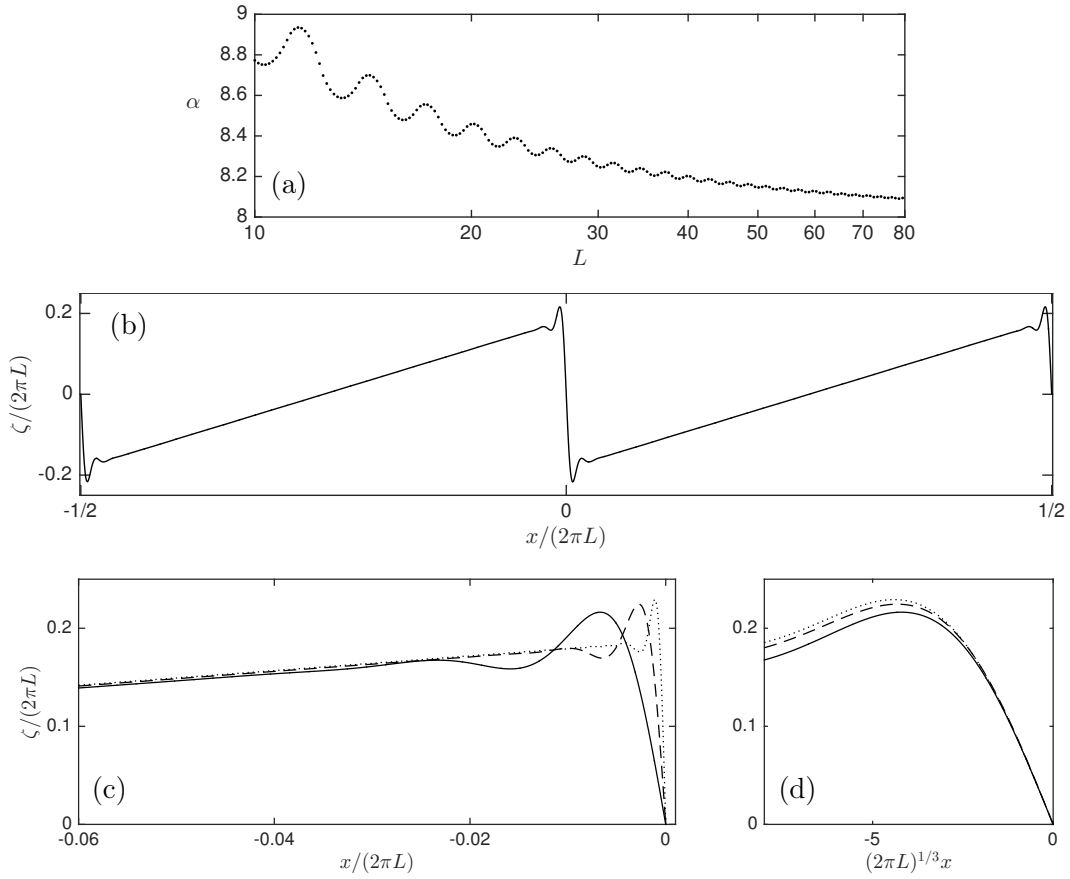


Figure 6: Optimal coefficients α and functions $\zeta(x)$ for the background method (18) with various L , computed by solving the truncated optimization (35) with $N \geq 8L$ modes. Displayed quantities are (a) optimal α for domains of various size $2\pi L$, (b) optimal $\zeta(x)$ for $L = 10^{1.3}$, and (c-d) details of optimal $\zeta(x)$ for $L = 10^{1.3}$ (—), $10^{1.6}$ (---), and $10^{1.9}$ (····).

- [6] P. Collet, J. P. Eckmann, H. Epstein, and J. Stubbe. A global attracting set for the Kuramoto–Sivashinsky equation. *Commun. Math. Phys.*, 152:203–214, 1993.
- [7] P. Constantin and C. R. Doering. Variational bounds on energy dissipation in incompressible flows: Shear flow. *Phys. Rev. E*, 49:4087–4099, 1994.
- [8] P. Constantin and C. R. Doering. Variational bounds on energy dissipation in incompressible flows. III. Convection. *Phys. Rev. E*, 53:5957–5981, 1996.
- [9] P. Cvitanović, R. L. Davidchack, and E. Siminos. On the state space geometry of the Kuramoto–Sivashinsky flow in a periodic domain. *SIAM J. Appl. Dyn. Syst.*, 9:1–33, 2010.
- [10] C. R. Doering and P. Constantin. Energy dissipation in shear driven turbulence. *Phys. Rev. Lett.*, 69:1648–1651, 1992.
- [11] A. Dooge, W. Govaerts, and Y. A. Kuznetsov. MatCont: A MATLAB package for numerical bifurcation analysis of ODEs. *ACM TOMS*, 29:141–164, 2003.
- [12] G. Fantuzzi, D. Goluskin, D. Huang, and S. I. Chernyshenko. Bounds for deterministic and stochastic dynamical systems using sum-of-squares optimization. *SIAM J. Appl. Dyn. Syst.*, 15:1962–1988, 2016.
- [13] G. Fantuzzi and A. Wynn. Construction of an optimal background profile for the Kuramoto–Sivashinsky equation using semidefinite programming. *Phys. Lett. A*, 379:23–32, 2015.
- [14] K. Gatermann and P. A. Parrilo. Symmetry groups, semidefinite programs, and sums of squares. *J. Pure Appl. Algebr.*, 192:95–128, 2004.
- [15] L. Giacomelli and F. Otto. New bounds for the Kuramoto–Sivashinsky equation. *Commun. Pure Appl. Math.*, 58:297–318, 2005.
- [16] M. Goldman, M. Josien, and F. Otto. New Bounds for the inhomogenous Burgers and the Kuramoto–Sivashinsky equations. *Commun. Partial Differ. Equations*, 40:2237–2265, 2015.
- [17] D. Goluskin. Bounding averages rigorously using semidefinite programming: mean moments of the Lorenz system. *J. Nonlinear Sci.*, In press, 2018.
- [18] D. Goluskin and C. R. Doering. Bounds for convection between rough boundaries. *J. Fluid Mech.*, 804:370–386, 2016.
- [19] J. Goodman. Stability of the Kuramoto–Sivashinsky and related systems. *Commun. Pure Appl. Math.*, 47:293–306, 1994.

- [20] P. J. Goulart and S. Chernyshenko. Global stability analysis of fluid flows using sum-of-squares. *Phys. D*, 241:692–704, 2012.
- [21] J. M. Greene and J. S. Kim. The steady states of the Kuramoto–Sivashinsky equation. *Phys. D*, 33:99–120, 1988.
- [22] D. Henrion and M. Korda. Convex computation of the region of attraction of polynomial control systems. *IEEE Trans. Automat. Contr.*, 59:297–312, 2014.
- [23] P. Holmes, J. L. Lumley, G. Berkooz, and W. Rowley. One-dimensional “turbulence”. In *Turbul. coherent Struct. Dyn. Syst. symmetry*, volume 15, chapter 8, pages 214–235. Cambridge University Press, Cambridge, UK, 2 edition, 2012.
- [24] P. J. Holmes, J. L. Lumley, G. Berkooz, J. C. Mattingly, and R. W. Wittenberg. Low-dimensional models of coherent structures in turbulence. *Phys. Rep.*, 287:337–384, 1997.
- [25] D. Huang, S. Chernyshenko, P. Goulart, D. Lasagna, O. Tutty, and F. Fuentes. Sum-of-squares polynomials approach to nonlinear stability of fluid flows: an example of application. *Proc. R. Soc. A*, 471:20150622, 2015.
- [26] J. M. Hyman and B. Nicolaenko. The Kuramoto–Sivashinsky equation: A bridge between PDE’s and dynamical systems. *Phys. D*, 18:113–126, 1986.
- [27] J. M. Hyman, B. Nicolaenko, and S. Zalesky. Order and complexity in the Kuramoto–Sivashinsky model of weakly turbulent interfaces. *Phys. D*, 23:265–292, 1986.
- [28] C. Jansson. VSDP: a MATLAB software package for verified semidefinite programming. Technical report, Hamburg University of Technology, 2006.
- [29] Y. Kuramoto and T. Tsuzuki. On the formation of dissipative structures in reaction-diffusion systems: reductive perturbation approach. *Progr. Theor. Phys.*, 54:687–699, 1975.
- [30] Y. Kuramoto and T. Tsuzuki. Persistent propagation of concentration waves in dissipative media far from thermal equilibrium. *Progr. Theor. Phys.*, 55:356–369, 1976.
- [31] J. B. Lasserre. Convergent SDP relaxations in polynomial optimization with sparsity. *SIAM Journal on Optimization*, 17(3):822–843, 2006.
- [32] J. Löfberg. YALMIP: a toolbox for modeling and optimization in MATLAB. In *IEEE Int. Conf. Comput. Aided Control Syst. Des.*, pages 284–289, Taipei, Taiwan, 2004.
- [33] J. Löfberg. Pre- and post-processing sum-of-squares programs in practice. *IEEE Trans. Automat. Contr.*, 54:1007–1011, 2009.

- [34] D. Michelson. Steady solutions of the Kuramoto–Sivashinsky equation. *Phys. D*, 19:89–111, 1986.
- [35] D. M. Michelson and G. I. Sivashinsky. Nonlinear analysis of hydrodynamic instability in laminar flames—II. Numerical experiments. *Acta Astronaut.*, 4:1207–1221, 1977.
- [36] MOSEK ApS. The MOSEK optimization toolbox for MATLAB manual. Version 7.1 (Revision 54), 2015.
- [37] K. G. Murty and S. N. Kabadi. Some NP-complete problems in quadratic and nonlinear programming. *Math. Program.*, 39:117–129, 1987.
- [38] R. Nicodemus, S. Grossmann, and M. Holthaus. Improved variational principle for bounds on energy dissipation in turbulent shear flow. *Phys. D Nonlinear Phenom.*, 101:178–190, 1997.
- [39] B. Nicolaenko, B. Scheurer, and R. Temam. Some global dynamical properties of the Kuramoto–Sivashinsky equations: nonlinear stability and attractors. *Phys. D*, 16:155–183, 1985.
- [40] B. O’Donoghue, E. Chu, N. Parikh, and S. Boyd. Conic optimization via operator splitting and homogeneous self-dual embedding. *Journal of Optimization Theory and Applications*, 169:1042–1068, June 2016.
- [41] B. O’Donoghue, E. Chu, N. Parikh, and S. Boyd. SCS: Splitting conic solver, version 2.0.2, November 2017.
- [42] F. Otto. Optimal bounds on the Kuramoto–Sivashinsky equation. *J. Funct. Anal.*, 257:2188–2245, 2009.
- [43] A. Papachristodoulou and S. Prajna. On the construction of Lyapunov functions using the sum of squares decomposition. In *Proc. 41st IEEE Conf. Decis. Control 2002*, volume 3, pages 3482–3487, 2002.
- [44] D. T. Papageorgiou and Y. S. Smyrlis. The route to chaos for the Kuramoto–Sivashinsky equation. *Theor. Comput. Fluid Dyn.*, 3:15–42, 1991.
- [45] D. Papp and S. Yildiz. Sum-of-squares optimization without semidefinite programming. *arXiv:1712.01792v1*, 2017.
- [46] P. A. Parrilo. *Structured semidefinite programs and semialgebraic geometry methods in robustness and optimization*. PhD thesis, California Institute of Technology, 2000.
- [47] P. A. Parrilo. Polynomial optimization, sums of squares, and applications. In G. Blekherman, P. A. Parrilo, and R. R. Thomas, editors, *Semidefinite optimization and convex algebraic geometry*, chapter 3, pages 47–157. SIAM, 2013.

- [48] S. C. Plasting and R. R. Kerswell. Improved upper bound on the energy dissipation rate in plane Couette flow: the full solution to Busse's problem and the Constantin–Doering–Hopf problem with one-dimensional background field. *J. Fluid Mech.*, 477:363–379, 2003.
- [49] Y. Pomeau, A. Pumir, and P. Pelce. Intrinsic stochasticity with many degrees of freedom. *J. Stat. Phys.*, 37:39–49, 1984.
- [50] G. I. Sivashinsky. Nonlinear analysis of hydrodynamic instability in laminar flames—I. Derivation of basic equations. *Acta Astronautica*, 4:1177–1206, 1977.
- [51] G. I. Sivashinsky and D. M. Michelson. On irregular wavy flow of a liquid film down a vertical plane. *Progr. Theor. Phys.*, 63:2112–2114, 1980.
- [52] I. Tobasco. (personal communication).
- [53] I. Tobasco, D. Goluskin, and C. R. Doering. Optimal bounds and extremal trajectories for time averages in dynamical systems. *Phys. Lett. A*, 382:382–386, 2018.
- [54] H. Waki, S. Kim, M. Kojima, and M. Muramatsu. Sums of squares and semidefinite program relaxations for polynomial optimization problems with structured sparsity. *SIAM Journal on Optimization*, 17:218–242, 2006.
- [55] R. W. Wittenberg. Optimal parameter-dependent bounds for Kuramoto–Sivashinsky-type equations. *Discret. Contin. Dyn. Syst.*, 34:5325–5357, 2014.
- [56] R. W. Wittenberg and P. Holmes. Scale and space localization in the Kuramoto–Sivashinsky equation. *Chaos*, 9:452–465, 1999.